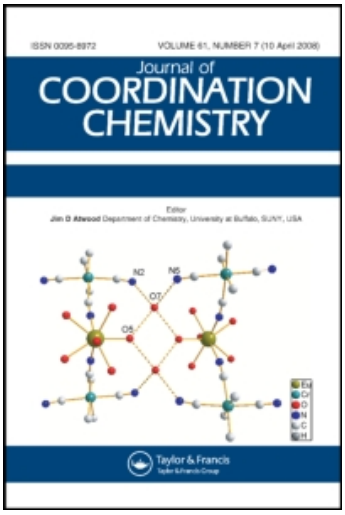

Journal of Coordination Chemistry
Publication details, including instructions for authors and subscription information:
http://www.informaworld.com/smpp/title~content=t713455674

Complexation of 4-amino-1,3 dimethyl-2,6 pyrimidine-dione derivatives with cobalt(II) and nickel(II) ions: synthesis, spectral, thermal and antimicrobial studies

Zeinab H. Abd El-Wahab[a]
[a] Faculty of Science (Girl's), Chemistry Department, Nasr City, Cairo, Egypt

To cite this Article Abd El-Wahab, Zeinab H.(2008) 'Complexation of 4-amino-1,3 dimethyl-2,6 pyrimidine-dione derivatives with cobalt(II) and nickel(II) ions: synthesis, spectral, thermal and antimicrobial studies', Journal of Coordination Chemistry, 61: 11, 1696 — 1709
To link to this Article: DOI: 10.1080/00958970701763076
URL: http://dx.doi.org/10.1080/00958970701763076

Journal of Coordination Chemistry
Vol. 61, No. 11, 10 June 2008, 1696–1709

Taylor & Francis
Taylor & Francis Group

Complexation of 4-amino-1,3 dimethyl-2,6 pyrimidine-dione derivatives with cobalt(II) and nickel(II) ions: synthesis, spectral, thermal and antimicrobial studies

ZEINAB H. ABD EL-WAHAB*

Faculty of Science (Girl's), Chemistry Department, Al-Azhar University, Nasr City, Cairo, Egypt, P.O. Box 11754

(*Received 17 April 2007; in final form 17 July 2007*)

Four heterocyclic Schiff-base ligands derived from condensation of 4-amino-1,3 dimethyl-2,6 pyrimidine-dione with 2-hydroxybenzaldehyde, 2-methoxybenzaldehyde, 4-hydroxy-3-methoxybenzaldehyde and 4-(dimethylamino) benzaldehyde, (HL^1, L^2, HL^3 and L^4), respectively, and their Co(II) and Ni(II) complexes have been prepared and characterized via elemental analysis, molar conductance, magnetic moment, thermal and XRPD analysis as well as spectral data (IR, ^{1}H-NMR, mass and solid reflectance). IR data reveal that the ligands are bidentate neutral ligands except HL^1, which is monobasic tridentate with coordination sites azomethine (N), carbonyl (O) and phenolic (O). Conductance data suggest that all complexes are non-electrolytes, except cobalt(II) complexes of L^2 and HL^3 are 1 : 1 electrolytes. The mass spectra confirm the proposed structure of the ligands and their complexes. The solid reflectance spectral data and magnetic moment measurements suggest octahedral, tetrahedral and square planar geometrical structures for the metal complexes. The spectral data were utilized to compute the important ligand field parameters B, β and D_q; LFSE also was calculated. The thermal behavior is also studied. Antibacterial and antifungal properties of the ligands and their complexes show broad-spectrum activities and the metal complexes show higher activity than the free ligands.

Keywords: Heterocyclic Schiff-base ligands; Metal complexes; Electronic spectra; Biological study

1. Introduction

Pyrimidine derivatives constitute a very important class of compounds because they are components of nucleic acids and have been shown to exert a pronounced physiological effect [1, 2]. The pyrimidine ring represents one constituent of nucleic acid, vitamins, coenzymes and antibiotics and provides potential binding sites for metal ions. The coordination properties of pyrimidines are important in understanding the role of metal ions in biological systems [3]. Metal complexes of purines, pyrimidines and their nucleotides play a dominant role in many biochemical systems: complexes of Co(III) and Cr(III) with nucleotides and their derivatives are useful for determining the

*Email: zhabdelwahab@yahoo.com

ISSN 0095-8972 print/ISSN 1029-0389 online © 2008 Taylor & Francis
DOI: 10.1080/00958970701763076

points where enzymes are activated or inhibited, platinum group metal complexes with purines, pyrimidines and nucleic acids possess antitumor and antibacterial activity [4], moreover some divalent transition metal complexes (Cu^{2+}, Zn^{2+}, Cd^{2+}, Co^{2+}, Hg^{2+}, UO_2^{2+}, *etc.*) of pyrimidine play an important role in maintaining functionalities of DNA, as well as being used in the preparation of pesticides [5].

In continuation of our studies on the synthesis and characterization of biologically-active complexes [6–11], this investigation includes the synthesis of cobalt and nickel complexes of a series of ligands:

- 4-(2-hydroxybenzylideneamino)-1,3dimethyl-2,6pyrimidine-dione, (HL^1)
- 4-(2-methoxybenzylideneamino)-1,3dimethyl-2,6pyrimidine-dione, (L^2)
- 4-(-3-methoxy-4-hydroxybenzylideneamino)-1,3dimethyl-2,6pyrimidine-dione, (HL^3) and
- 4-{4-(dimethylamino)benzylideneamino}-1,3dimethyl-2,6pyrimidine-dione, (L^4)

The structural chemistry of these ligands and their complexes with Co(II) and Ni(II) are examined via different physicochemical tools such as elemental analysis, IR, ^{1}H-NMR and mass spectra, magnetic moment, molar conductance, XRPD, thermal analyses, and solid reflectance spectral techniques. Furthermore, all synthesized compounds were screened for their antimicrobial activity in attempt to understand the influence of metal ion and ligand nature on the biological properties.

2. Experimental

2.1. *Analysis and physical measurements*

All chemicals used were of highest available purity. They include 4-amino-1,3 dimethyl-2,6 pyrimidine-dione (Aldrich), 2-hydroxybenzaldehyde, 2-methoxybenzaldehyde, 4-hydroxy-3-methoxybenzaldehyde, and 4-(dimethylamino) benzaldehyde (Sigma), cobalt and nickel chloride hexahydrates (BDH). Solvents, absolute ethyl alcohol, diethylether, dimethylformamide (DMF) and dimethylsulfoxide (DMSO) were purchased from Merck or Sigma. Concentrated nitric and perchloric acid were reagent grade and used as supplied.

Carbon, hydrogen and nitrogen contents were determined using a Perkin-Elmer 2408 CHN analyzer. Metal contents were determined by titration against standard EDTA solution and the chloride contents were determined gravimetrically [12]. Melting or decomposition points were carried out on a melting point apparatus, Gallenkamp, England. IR spectra were recorded on a Perkin-Elmer FT-IR type 1650 spectrophotometer using KBr discs. ^{1}H-NMR spectra were recorded using a Bruker ARX-300 spectrometer using DMSO-d_6 as a solvent, chemical shifts are reported in parts per million downfield from tetramethylsilane. Mass spectra were recorded on a Jeol JMSAX-500 mass spectrometer. Electronic spectra of solutions of all ligands in DMF and the solid reflectance spectra of their complexes were recorded on a Jasco model V-550 UV-vis spectrophotometer. Magnetic susceptibility of the metal complexes were measured by the Gouy method at room temperature using a Johnson Matthey, Alpha products, model MKI magnetic susceptibility balance and the effective magnetic moments were calculated using the relation $\mu_{eff} = 2.828$

$(\chi_m \cdot T)^{1/2}$ B.M., where χ_m is the molar susceptibility corrected using Pascal's constants for diamagnetism of all atoms in the compounds. The molar conductance measurements were measured in solutions of the metal complexes in DMF (10^{-3} M) using WTWD-812 Weilheium-Conductivity meter model LBR, fitted with a cell model LTA100. A Shimadzu TGA-50H thermal analyzer was used to record simultaneously the TG and DTG curves; the experiments were carried out in dynamic nitrogen atmosphere (20 ml Min^{-1}) with a heating rate 10°C min^{-1} in the temperature range 20–1000°C using platinum crucibles. Highly sintered α-Al_2O_3 was used as a reference. X-ray powder diffraction analysis of all ligands and their complexes were carried out at ambient temperature with a Shimadzu 160D X-ray diffractometer using Cu-Kα radiation over the range ($4 < 2\theta < 80$), with steps of 0.01° and a step time of 2 s. The antimicrobial activity of the ligands and their complexes were screened using the diffusion method [11].

2.2. *Ligand syntheses*

All Schiff-base ligands under study (HL^1, L^2, HL^3 and L^4) were prepared by adding a solution of 2-hydroxybenzaldehyde, 2-methoxybenzaldehyde, 4-hydroxy-3-methoxy-benzaldehyde, or 4-(dimethylamino) benzaldehyde (0.1 mol) in ethanol, respectively, to 4-amino-1,3 dimethyl-2,6 pyrimidine-dione (0.1 mole) in the same solvent in presence of few drops of piperidine. The mixture was kept under reflux for 4 h on a water bath and then allowed to cool to room temperature. The product was filtered off, recrystallized from ethanol and dried in a desiccator over anhydrous calcium chloride. The reaction route for the ligand syntheses and their structures, names and abbreviations are given in scheme 1.

2.3. *Metal complexes synthesis*

A solution of $CoCl_2 \cdot 6H_2O$ or $NiCl_2 \cdot 6H_2O$ dissolved in ethanol was added gradually to a stirred ethanolic solution of the Schiff base (HL^1, L^2, HL^3 and L^4) in the molar ratio 1:1. The reaction mixture was further stirred for 3 h to ensure complete precipitation of the formed complexes. The precipitated complexes were filtered, washed several times with 50% (v/v) ethanol-water to remove any unreacted starting materials, followed by diethylether and dried in a vacuum desiccator over anhydrous calcium chloride. All complexes are colored powders stable in air and insoluble in common organic solvents, but soluble in DMF and DMSO. The elemental analysis and some physico-chemical characteristics for all ligands and their complexes are collected in table 1.

3. Results and discussion

Condensation of the aldehydes with amine readily gives rise to Schiff-base ligands which were easily identified by their IR, ^{1}H–NMR and mass spectra. Their reactions with Co(II) and Ni(II) afford mononuclear metal complexes in which the

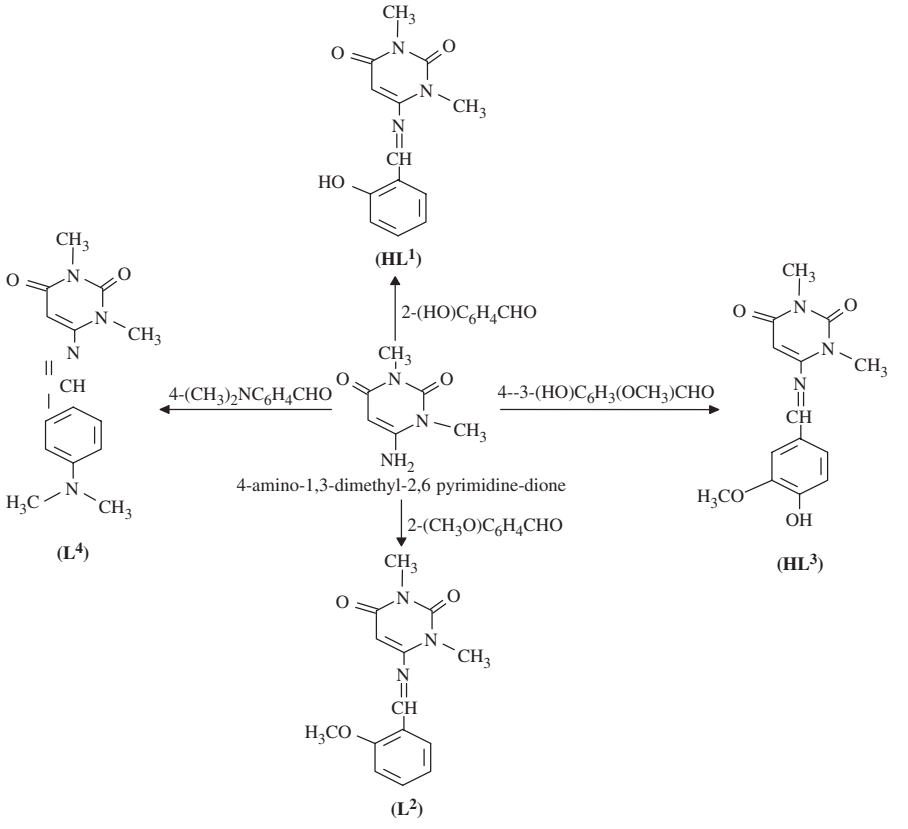

Scheme 1. Synthetic route to the Schiff-base ligands under study.
HL[1]: 4-(2-hydroxybenzylideneamino)-1,3-dimethyl-2,6 pyrimidine-dione.
L[2]: 4-(2-methoxybenzylideneamino)-1,3-dimethyl-2,6 pyrimidine-dione.
HL[3]: 4-(3-methoxy-4-hydroxybenzylideneamino)-1,3-dimethyl-2,6 pyrimidine-dione.
L[4]: 4-[4-(dimethylamino)benzylideneamino]-1,3-dimethyl-2,6 pyrimidine-dione.

microanalytical data as well as metal and chloride estimations are in good agreement with proposed stoichiometries (table 1). The reactions follow:

$$\mathbf{HL^1 + MCl_2 \cdot 6H_2O \rightarrow [ML^1Cl \cdot 2H_2O] \cdot \tfrac{1}{2}H_2O + 3.5H_2O}$$
$$\mathrm{M = Co(II); Ni(II)}$$
$$\mathbf{L^2 + MCl_2 \cdot 6H_2O \rightarrow [ML^2X]y + z}$$
$$\mathrm{M = Co(II); X = Cl \cdot H_2O;}\ y = \mathrm{Cl \cdot H_2}O;\ \mathrm{z = 4H_2O}$$
$$\mathrm{Ni(II); X = 2Cl \cdot 2H_2O; y = 1\tfrac{1}{4}H_2O; z = 2\tfrac{3}{4}H_2O}$$
$$\mathbf{HL^3 + MCl_2 \cdot 6H_2O \rightarrow [M(HL^3)X]y + z}$$
$$\mathrm{M = Co(II); X = Cl \cdot H_2O; y = Cl \cdot \tfrac{1}{2}H_2O; z = 4\tfrac{1}{2}H_2O}$$
$$\mathrm{Ni(II); X = 2Cl \cdot 2H_2O; y = \tfrac{1}{2}H_2O; z = 3\tfrac{1}{2}H_2O}$$
$$\mathbf{L^4 + MCl_2 \cdot 6H_2O \rightarrow [ML^4X]y + z}$$
$$\mathrm{M = Co(II); X = 2Cl \cdot 2H_2O; y = 2\tfrac{1}{4}H_2O; z = 1\tfrac{3}{4}H_2O}$$
$$\mathrm{Ni(II); X = 2Cl; y = \tfrac{1}{2}H_2O; z = 5\tfrac{1}{2}H_2O}$$

Table 1. Analytical data and some physical properties for Schiff-base ligands and their metal complexes.

Compound No. Empirical formula	M.wt. Found (Calcd)[a]	Color	M.P. (°C)	Λ_m^b	μ_{eff}(B.M.)[c]	Elemental analysis, found (Calcd%) C	H	N	Cl	M
HL^1; $C_{13}H_{13}N_3O_3$	258.00 (259.29)	Pale orange	182	–	–	60.00 (60.21)	5.27 (5.06)	16.34 (16.21)	–	–
$[CoL^1Cl(H_2O)_2]\cdot\frac{1}{2}H_2O$; $CoC_{13}H_{12}N_3O_3Cl\cdot2\frac{1}{2}H_2O$	396.00 (397.71)	Pink	289	10.11	4.94	39.00 (39.26)	4.33 (4.32)	10.81 (10.57)	8.95 (8.91)	14.84 (14.82)
$[NiL^1Cl(H_2O)_2]\cdot\frac{1}{2}H_2O$; $NiC_{13}H_{12}N_3O_3Cl\cdot2\frac{1}{2}H_2O$	399.00 (397.47)	Pale green	257	3.00	3.02	39.29 (39.28)	4.27 (4.32)	10.69 (10.57)	9.00 (8.92)	14.38 (14.77)
L^2; $C_{14}H_{15}N_3O_3$	273.00 (273.32)	Pale yellow	290	–	–	61.54 (61.52)	5.70 (5.54)	15.33 (15.38)	–	–
$[CoL^2Cl(H_2O)]Cl\cdot H_2O$; $CoC_{14}H_{15}N_3O_3Cl_2\cdot2H_2O$	438.00 (439.19)	Pale blue	266	74.35	4.76	38.21 (38.28)	4.75 (4.37)	9.62 (9.57)	16.39 (16.14)	13.66 (13.42)
$[NiL^2(Cl)_2(H_2O)_2]\cdot1\frac{1}{4}H_2O$; $NiC_{14}H_{15}N_3O_3Cl_2\cdot3\frac{1}{4}H_2O$	460.00 (461.48)	Green	>300	3.82	2.99	36.01 (36.43)	4.66 (4.71)	9.15 (9.11)	15.24 (15.36)	13.00 (12.72
HL^3; $C_{14}H_{15}N_3O_4$	288.00 (289.32)	Pink	155	–	–	58.33 (58.12)	5.39 (5.24)	14.61 (14.53)	–	–
$[Co(HL^3)Cl(H_2O)]Cl\cdot\frac{1}{2}H_2O$; $CoC_{14}H_{15}N_3O_4Cl_2\cdot1\frac{1}{2}H_2O$	445.00 (446.18)	Bluish green	242	83.15	4.69	38.09 (37.68)	3.85 (4.07)	9.37 (9.42)	16.05 (15.89)	13.00 (13.21)
$[Ni(HL^3)(Cl)_2(H_2O)_2]\cdot\frac{1}{2}H_2O$; $NiC_{14}H_{15}N_3O_4Cl_2\cdot2\frac{1}{2}H_2O$	463.00 (463.96)	Greenish blue	269	5.05	3.20	36.06 (36.24)	4.38 (4.35)	8.99 (9.06)	14.99 (15.28)	12.54 (12.65)
L^4; $C_{15}H_{18}N_4O_2$	286.00 (286.37)	Yellow	241	–	–	62.99 (62.91)	6.19 (6.35)	19.38 (19.57)	–	–
$[CoL^4(Cl)_2(H_2O)_2]\cdot2\frac{1}{4}H_2O$; $CoC_{15}H_{18}N_4O_2Cl_2\cdot4\frac{1}{4}H_2O$	493.00 (492.79)	Dark red	>300	13.03	4.89	36.31 (36.56)	5.76 (5.43)	11.61 (11.37)	14.19 (14.39)	11.97 (11.96)
$[NiL^4(Cl)_2]\cdot\frac{1}{2}H_2O$; $NiC_{15}H_{18}N_4O_2Cl_2\cdot\frac{1}{2}H_2O$	425.00 (424.97)	Brown	277	12.12	diamag.	42.44 (42.39)	4.61 (4.52)	13.00 (13.19)	16.82 (16.68)	13.79 (13.81)

L^1 represents the deprotonated form of HL^1 ligand.
[a]Found values obtained from mass spectra.
[b]Molar conductance ($Ohm^{-1}cm^2mol^{-1}$) of 1×10^{-3} M solution in DMF at room temperature.
[c]Room temperature effective magnetic moment.

3.1. *IR spectra and mode of bonding*

The main IR bands were compared with those of the free ligands (table 2). The infrared spectra of all ligands under study showed the following: (1) No characteristic absorption assignable to NH_2 function indicating formation of Schiff base supported by appearance of a strong sharp band in the 1625–1620 cm^{-1} region due to azomethine linkage as reported for similar ligands [13, 14]. (2) The observation of strong bands at 1670–1666 cm^{-1} and 1744–1696 cm^{-1} due to νC(2)=O and νC(6)=O stretching vibrations of carbonyl mode [3, 15–17]. (3) A broad band at 3398 and 3430 cm^{-1} was observed in the spectra of HL^1 and HL^3, respectively, attributed to phenolic O–H group [17, 18], and a strong band observed at 1273 cm^{-1} and 1306 cm^{-1} in the same ligands has been assigned to ν(C–O) mode of phenolic group [14, 19, 20]. All ligands display characteristic stretching absorption bands due to the pyrimidine ring at 3060–3056 cm^{-1}, and the phenyl group shows C–H stretching at 3032–3030 cm^{-1} [13].

Comparison of IR spectra of the ligands and their metal complexes brings out the following: (1) The azomethine stretch shifted in the spectra of all complexes to lower energy compared to the free ligands with the appearance of a vibration at 498–462 cm^{-1} corresponding to M–N, confirming involvement of the azomethine nitrogen in complex formation [15]. (2) The position and intensity of $\nu(C_6{=}O)$ of the free ligands change appreciably during complexation to lower energy, 1691–1670 cm^{-1}. This indicates that carbonyl oxygen is involved in the complexes, while there is little change in $\nu(C_2{=}O)$ ruling out its coordination [1, 16]. (3) The disappearance of the band attributed to ν(O–H) in the ligand, HL^1 on complexation with metal ions indicates deprotonation prior to coordination through oxygen. (4) A medium intensity band around 532–500 cm^{-1} assignable for ν(M–O) also supports oxygen coordination [18]. Participation of the OH group in coordination is further confirmed by the lowering in the phenolic C–O stretch compared to the free ligand. (5) The presence of a broad band at 3500–3360 cm^{-1} for the solid complexes is associated with stretching modes of coordinated and/or lattice water molecules supported from thermal analysis study [21].

3.2. *^{1}H-NMR spectra*

The ^{1}H-NMR spectra of all ligands under study in DMSO-d_6 do not show a signal corresponding to the primary amine, supporting the complete condensation and formation of imine product. The assignment of ^{1}H-NMR spectra of the Schiff-base ligands is listed in table 2. All free ligands show signals due to azomethine at $\delta = 8.61$–8.38 (s, 1H) ppm providing evidence for formation of Schiff base [15]. The aromatic protons are observed as complex multiplets between $\delta = 7.88$–6.71 ppm [13, 14]. The signals at $\delta = 5.89$–5.33 ppm and at $\delta = 3.40$–3.23 ppm are due to C(5)-H of pyrimidine ring and (s, 3H, NCH_3), respectively [15, 22]. The ligands, HL^1 and HL^3, show signals due to the phenolic proton at $\delta = 9.90$ and 10.30 (s, 1H) ppm [13, 14], while L^2 and HL^3 show signals due to methoxy at $\delta = 3.60$ and 3.70 (s, 3H) ppm [23]. The observed signals at $\delta = 3.27$ ppm in the spectrum of L^4 are due to {s, 3H, $N(CH_3)_2$} [24].

3.3. *Conductivity measurements*

The conductance measurements recorded for 10^{-3} M solutions of the metal complexes in DMF are listed in table 1. All complexes, except two, are non-conducting from

Table 2. Main IR and ^{1}H NMR data with their assignment for Schiff-base ligands and their Co(II) and Ni(II) complexes.

Compound No.	IR bands (cm^{-1}) ν_{O-H} (pheno.)	$\nu_{C(6)=O}$ (carbo.)	$\nu_{C=N}$ (azome.)	ν_{C-O} (pheno.)	ν_{M-O}	ν_{M-N}	^{1}H-NMR (δ, ppm)
HL^1	3398_{br}	1696_s	1620_{sh}	1273_s	–	–	9.90(s, OH), 8.51(s, HC=N), 7.45–6.72(m, phenyl proton), 5.33($C_{(5)}$–H), 3.23(s, N–CH_3)
$[CoL^1Cl(H_2O)_2]\cdot\frac{1}{2}H_2O$	–	1675_s	1580_{sh}	1252_s	532_m	492_m	–
$[NiL^1Cl(H_2O)_2]\cdot\frac{1}{2}H_2O$	–	1684_s	1596_{sh}	1216_s	530_m	462_m	–
L^2	–	1698_s	1622_{sh}	–	–	–	8.48(s, HC=N), 7.65–6.71(m, phenyl proton), 5.70($C_{(5)}$–H), 3.31(s, N–CH_3), 3.60(s, O–CH_3)
$[CoL^2Cl(H_2O)]Cl\cdot H_2O$	–	1690_s	1588_{sh}	–	513_m	490_m	–
$[NiL^2(Cl)_2(H_2O)_2]\cdot1\frac{1}{4}H_2O$	–	1676_s	1548_{sh}	–	528_m	486m	–
HL^3	3430_{br}	1744_s	1625_{sh}	1306_s	–	–	10.30(s, OH), 8.61(s, HC=N), 7.88–6.91(m, phenyl proton), 5.89($C_{(5)}$–H), 3.40(s, N–CH_3), 3.70(s, O–CH_3)
$[Co(HL^3)Cl(H_2O)]Cl\cdot\frac{1}{2}H_2O$	3428_{br}	1670_s	1504_{sh}	1305_s	522_m	466_m	–
$[Ni(HL^3)(Cl)_2(H_2O)_2]\cdot\frac{1}{2}H_2O$	3426_{br}	1675_s	1506_{sh}	1304_s	500_m	482_m	–
L^4	–	1716_s	1622_{sh}	–	–	–	8.38(s, HC=N), 7.15–6.77(m, phenyl proton), 5.69($C_{(5)}$–H), 3.36(s, N–CH_3), 3.27{s, N–$(CH_3)_2$}
$[CoL^4(Cl)_2(H_2O)_2]\cdot2\frac{1}{4}H_2O$	–	1705_s	1557_{sh}	–	504_m	468_m	–
$[NiL^4(Cl)_2]\cdot\frac{1}{2}H_2O$	–	1691_s	1546_{sh}	–	512_m	498_m	–

^{sh}sharp; ^{s}strong; ^{m}medium; ^{br}broad (IR data) and ^{s}singlet; ^{m}multiple (NMR data).

3.00 to 13.03 $Ohm^{-1}\,cm^2\,mol^{-1}$ indicating their neutrality, so the chloride is absent or inside the coordination sphere. The exceptions are cobalt complexes of L^2 and HL^3 which showed molar conductances of 74.35 and 83.15 $Ohm^{-1}\,cm^2\,mol^{-1}$, respectively, indicating 1 : 1 electrolyte [7, 14].

3.4. *Magnetic susceptibility measurements*

The room temperature effective magnetic moment values of the metal complexes are reported in table 1. Co(II) complexes have μ_{eff} values of 4.94–4.69 B.M., corresponding to three unpaired electrons but higher than the spin-only value (3.87) due to the orbital angular momentum contribution in a d^7-system. The magnetic moment values of the Ni(II) complexes, except one, lie in the range 3.20–2.99 B.M. corresponding to two unpaired electrons. The exception is Ni(II) complex from L^4 that displays diamagnetic behavior [6, 25].

3.5. *Electronic spectra measurements*

The electronic absorption spectra of the free Schiff base in DMF displayed two absorption bands in the region $(29.41–27.40) \times 10^3\,cm^{-1}$ and $(36.36–33.33) \times 10^3\,cm^{-1}$, which are assigned to π–π^* and n–π^* transitions involving the molecular orbitals of the C=N and both benzene and pyrimidine rings. Upon complexation, these transitions shifted to lower or higher energy regions compared to the free ligands confirming coordination of the ligands to metal, in addition to appearance of new bands at longer wavelength assigned to LMCT and d-d transitions [14, 18].

The electronic spectra of cobalt(II) complexes derived from HL^1 and L^4 exhibit two bands, $(14.93–14.79) \times 10^3\,cm^{-1}$ and $(18.66–18.62) \times 10^3\,cm^{-1}$, assignable to $^4T_{1g}(F) \rightarrow {}^4A_{2g}(F)$ (υ_2) and $^4T_{1g}(F) \rightarrow {}^4T_{1g}(P)$ (υ_3) in addition to another band at $(28.57–26.32) \times 10^3\,cm^{-1}$ from charge transfer suggest octahedral geometry [21, 26]. The value of magnetic moments (4.94–4.89 B.M.) is in good agreement with those reported for octahedral [27]. However, the cobalt(II) complexes from L^2 and HL^3 exhibit one main band at ca $(16.20–15.69) \times 10^3\,cm^{-1}$ due to $^4A_2(F) \rightarrow {}^4T_1(P)$ (υ_3) suggesting tetrahedral geometry [28]. The values of magnetic moments (4.76–4.69 B.M.) are also evidence for tetrahedral geometry [27].

The nickel(II) complexes of HL^1, L^2 and HL^3 are paramagnetic precluding square planar configuration. Their spectra show three electronic bands in regions $(12.72–12.64) \times 10^3\,cm^{-1}$, $(19.33–18.99) \times 10^3\,cm^{-1}$ and $(23.89–22.96) \times 10^3\,cm^{-1}$ due to $^3A_{2g}(F) \rightarrow {}^3T_{2g}(F)$ (υ_1), $^3A_{2g}(F) \rightarrow {}^3T_{1g}(F)$ (υ_2) and $^3A_{2g}(F) \rightarrow {}^3T_{1g}(P)$ (υ_3) transition suggesting high-spin octahedral Ni(II); the band at $(29.91–29.00) \times 10^3\,cm^{-1}$ is from charge transfer [21]. The measured magnetic moments, 3.20–2.99 B.M., fall in the range reported for octahedral. The Ni(II) complex of L^4 displays two bands at *ca* $16.80 \times 10^3\,cm^{-1}$ and $21.74 \times 10^3\,cm^{-1}$ due to the transition $^1A_{1g}(D) \rightarrow {}^1A_{2g}(G)$ (υ_1) and $^1A_{1g}(D) \rightarrow {}^1B_{2g}(G)$ (υ_2) suggesting square planar Ni(II); its diamagnetism supports the suggested structure [15, 29].

Various ligand field parameters (D_q, B and β) in addition to LFSE were calculated for the octahedral Co(II) and Ni(II) complexes. The parameters ($10\,D_q$) and (B) have been calculated from (υ_2) and (υ_3) for Co(II) while in Ni(II) complexes, (υ_1) directly gives the value of ($10\,D_q$) [30]. A summary of the electronic spectra and ligand field

parameters collected are given in table 3 and agree well with those reported for similar complexes.

3.6. *Mass spectra*

The mass spectra of the free ligands and complexes show molecular ion peaks; both the calculated and found values of their molecular weights are given in table 1. Also, the mass spectra show numerous peaks representing successive degradation of the complexes molecules corresponding to various fragments, their intensity gives an idea on the stability of the fragments. Schemes 2–4 (supplementary data available online) demonstrate the proposed paths of the decomposition steps for some ligands and complexes as representative example, while figures 1–3 (supplementary data available online) show representative mass spectra for some ligands and complexes.

3.7. *Thermal analysis*

The decomposition stages, temperature range, decomposition product as well as the found and calculated weight loss temperatures of the metal complexes are given in table 4.

Details are provided for $[CoL^1Cl(H_2O)_2]\cdot \tfrac{1}{2}H_2O$ and $[NiL^1Cl(H_2O)_2]\cdot \tfrac{1}{2}H_2O$ as examples which undergo decomposition in five stages. The first stage takes place in the 40–120°C range corresponding to release of $\tfrac{1}{2}H_2O$ (hydrated) from each complex with weight losses of 2.93 and 1.40%, respectively (calculated 2.27%). The second decomposition stage occurs in the 100–230°C range with mass loss of 14.70 and 11.00% (calculated 14.85 and 11.33%) that correlate with elimination of $2H_2O$ and $\tfrac{1}{2}N_2$ for the first complex and only $2H_2O$ (coordinated) for the second complex. The third stage occurs in the 230–330°C range corresponding to loss of N_2, O_2 and $\tfrac{1}{2}Cl_2$ for the first complex and $\tfrac{1}{2}N_2$, $\tfrac{1}{2}Cl_2$ and 2NO for the second complex with mass loss of 39.00 and 38.90% (calculated 38.85 and 38.88%, respectively). The fourth decomposition stage takes place from 320–450° with weight loss of 65.40 and 66.00% (calculated 65.54 and 65.58%) corresponding to loss of CO and C_6H_6. The final decomposition stage takes place in the 423–519 and 447–565°C ranges, respectively, with weight loss of 85.30 and 86.00% (calculated 85.18 and 85.23%) that correlate with the loss of $3C_2H_2$ from each complex and formation of Co and Ni metals as residue. Details for the other complexes are found in the supplementary data available online.

3.8. *X-ray powder diffraction study*

X-ray powder diffraction patterns of all ligands and their complexes were recorded between 4° and 80° (2θ). The value of (2θ), interplanar spacing d(°A) and the relative intensities (I/I^0) of the compounds under study were recorded in table 1s (supplementary data available online). By comparing the X-ray chart of each ligand with its corresponding metal complexes, it is concluded that the interplanar spacing, d(°A) and the relative intensities (I/I^0) are different, which could be attributed to the complex formation.

Table 3. Electronic parameters of cobalt(II) and nickel(II) complexes*.

Compound No.	Suggested structure	Absorption bands (cm^{-1})/peak assignment			D_q (cm^{-1})	B (cm^{-1})	β	β%	LFSE (cm^{-1})
		υ_1	υ_2	υ_3					
$[CoL^1Cl(H_2O)_2]\cdot\frac{1}{2}H_2O$	Octahedral		14.79×10^3	18.66×10^3	791	854	0.76	23.75	6.33×10^3
$[CoL^4(Cl)_2(H_2O)_2]\cdot 2\frac{1}{4}H_2O$	Octahedral		14.93×10^3 $^4T_{1g}(F)\rightarrow{}^4A_{2g}(F)$	18.62×10^3 $^4T_{1g}(F)\rightarrow{}^4T_{1g}(P)$	798	847	0.76	24.38	6.39×10^3
$[CoL^2Cl(H_2O)]Cl\cdot H_2O$	Tetrahedral			15.69×10^3					
$[Co(HL^3)Cl(H_2O)]Cl\cdot\frac{1}{2}H_2O$	Tetrahedral			16.20×10^3 $^4A_2(F)\rightarrow{}^4T_1(P)$					
$[NiL^1Cl(H_2O)_2]\cdot\frac{1}{2}H_2O$	Octahedral	12.69×10^3	19.22×10^3	23.89×10^3	1269	740	0.69	31.48	15.23×10^3
$[NiL^2(Cl)_2(H_2O)_2]\cdot 1\frac{1}{4}H_2O$	Octahedral	12.72×10^3	19.33×10^3	23.25×10^3	1272	755	0.76	30.09	15.26×10^3
$[Ni(HL^3)(Cl)_2(H_2O)_2]\cdot\frac{1}{2}H_2O$	Octahedral	12.64×10^3 $^3A_{2g}(F)\rightarrow{}^3T_{2g}(F)$	18.99×10^3 $^3A_{2g}(F)\rightarrow{}^3T_{1g}(F)$	22.96×10^3 $^3A_{2g}(F)\rightarrow{}^3T_{1g}(P)$	1264	708	0.66	34.44	15.17×10^3
$[NiL^4(Cl)_2]\cdot\frac{1}{2}H_2O$	Square planar	16.80×10^3 $^1A_{1g}(D)\rightarrow{}^1A_{2g}(G)$	21.47×10^3 $^1A_{1g}(D)\rightarrow{}^1B_{2g}(G)$						

*The ligand field splitting energy (Dq), interelectronic repulsion parameter (B), nephelauxetic ratio (β) and ligand field stabilization energy (LFSE).
The lowering in the (B) values compared to the free metal ion values (1120 and 1080 for Co(II) andNi(II) ions, respectively) suggests appreciable amount of the covalent character in the metal-ligandbonds. Additionally, (β) value is less than unity suggesting a largely covalent bond between the organicligands and metal(II) ions in these complexes.

Table 4. Thermoanalytical results of Co(II) and Ni(II) complexes.

Complex compound	Stage	Temp. range (°C)	Mass loss% Calcd	Mass loss% Found	Evolved moiety	Residue
$[CoL^1Cl(H_2O)_2]\cdot\frac{1}{2}H_2O$	I	42–119	2.27	2.93	$\frac{1}{2}H_2O$ (hydr.)	$CoC_{13}H_{12}N_3O_3Cl\cdot 2H_2O$
	II	119–231	14.85	14.70	$2H_2O$ (coord.) and $\frac{1}{2}N_2$	$CoC_{13}H_{12}N_2O_3Cl$
	III	231–319	38.85	39.00	N_2, O_2 and $\frac{1}{2}Cl_2$	$CoC_{13}H_{12}O$
	IV	319–423	65.54	65.40	CO and C_6H_6	CoC_6H_6
	V	423–519	85.18	85.30	$3C_2H_2$	Co
$[NiL^1Cl(H_2O)_2]\cdot\frac{1}{2}H_2O$	I	50–104	2.27	1.40	$\frac{1}{2}H_2O$ (hydr.)	$NiC_{13}H_{12}N_3O_3Cl\cdot 2H_2O$
	II	104–229	11.33	11.00	$2H_2O$ (coord.)	$NiC_{13}H_{12}N_3O_3Cl$
	III	229–332	38.88	38.90	$\frac{1}{2}N_2$, $\frac{1}{2}Cl_2$ and 2NO	$NiC_{13}H_{12}O$
	IV	332–447	65.58	66.00	CO and C_6H_6	NiC_6H_6
	V	447–565	85.23	86.00	$3C_2H_2$	Ni
$[CoL^2Cl(H_2O)]Cl\cdot H_2O$	I	31–279	8.21	8.00	H_2O (hydr.) and H_2O (coord.)	$CoC_{14}H_{15}N_3O_3Cl_2$
	II	279–332	67.66	68.00	O_2, Cl_2, N_2, C_6H_6 and $2C_2H_2$	CoC_4H_5NO
	III	332–403	73.82	73.50	HCN	CoC_3H_4O
	IV	403–525	86.58	86.60	CO and C_2H_4	Co
$[NiL^2(Cl)_2(H_2O)_2]\cdot 1\frac{1}{4}H_2O$	I	27–80	15.18	14.86	$1\frac{1}{4}H_2O$ (hydr.), $1\frac{1}{4}H_2O$ (coord.), and $\frac{1}{2}O_2$	$NiC_{14}H_{15}N_3O_2Cl_2\cdot\frac{1}{4}H_2O$
	II	80–186	16.16	15.98	$\frac{1}{4}H_2O$ (coord.)	$NiC_{14}H_{15}N_3O_2Cl_2$
	III	186–400	65.06	64.50	O_2, N_2, $\frac{1}{2}Cl_2$, C_6H_6 and $2C_2H_2$	NiC_4H_5NCl
	IV	400–547	87.28	87.60	$\frac{1}{2}N_2$, HCl and $2C_2H_2$	Ni
$[Co(HL^3)Cl(H_2O)]Cl\cdot\frac{1}{2}H_2O$	I	48–108	1.01	1.03	$\frac{1}{4}H_2O$ (hydr.)	$CoC_{14}H_{15}N_3O_4Cl_2\cdot 1\frac{1}{4}H_2O$
	II	108–265	6.06	6.00	$\frac{1}{4}H_2O$ (hydr.) and H_2O (coord.)	$CoC_{14}H_{15}N_3O_4Cl_2$
	III	265–391	45.74	45.00	N_2, Cl_2 and C_6H_6	$CoC_8H_9NO_4$
	IV	391–547	83.21	83.00	3CO, HCN and $2C_2H_4$	CoO
$[Ni(HL^3)(Cl)_2(H_2O)_2]\cdot\frac{1}{2}H_2O$	I	29–90	0.97	0.15	$\frac{1}{4}H_2O$ (hydr.)	$NiC_{14}H_{15}N_3O_4Cl_2\cdot 2\frac{1}{4}H_2O$
	II	90–279	9.71	10.00	$\frac{1}{4}H_2O$ (hydr.) and $2H_2O$ (coord.)	$NiC_{14}H_{15}N_3O_4Cl_2$
	III	279–449	65.98	66.00	N_2, Cl_2, 3CO and C_6H_6	NiC_5H_9NO
	IV	449–518	83.90	84.00	HCN and $2C_2H_4$	NiO
$[CoL^4(Cl)_2(H_2O)_2]\cdot 2\frac{1}{4}H_2O$	I	30–314	29.93	30.00	$2\frac{1}{4}H_2O$ (hydr.), $2H_2O$ (coord.) and Cl_2	$CoC_{15}H_{18}N_4O_2$
	II	314–522	84.97	85.00	NO, 3CN, C_6H_6 and $3C_2H_4$	CoO
$[NiL^4(Cl)_2]\cdot\frac{1}{2}H_2O$	I	100–314	40.48	40.00	$\frac{1}{2}H_2O$ (hydr.), $\frac{1}{2}N_2$, Cl_2 and C_6H_6	$NiC_9H_{12}N_3O_2$
	II	314–497	82.42	83.00	$\frac{1}{2}O_2$, 3CN and $3C_2H_4$	NiO

3.9. *Antimicrobial assay*

The Schiff-base ligands and their metal complexes in addition to $CoCl_2 \cdot 6H_2O$ and $NiCl_2 \cdot 6H_2O$ were screened for antibacterial activity against two gram-positive bacterial strains (*Staphylococcus aureus* and *Bacillus anthracis*) and two gram-negative bacterial strains (*Escherichia coli* and *Pseudomonas aeruginosa*) as well as two fungal strains (*Candida albicans* and *Penicillium italicum*) using the diffusion method. The results are summarized in table 5 in addition to the calculated percent activity index data [31].

For the ligands:

- The highest antimicrobial activity was observed against bacteria strains.
- HL^1 was more effective against all types of bacteria and fungi than the other ligands; HL^3 displays the least activity.
- There was almost no difference in toxicity against bacteria and fungi among L^2, HL^3 and L^4.
- The activity of the ligands increased upon complexation with Co(II) and Ni(II); such increased activity of the complexes can be explained on the basis of Overtone's concept and chelation theory [32].

For comparison of the metal complexes:

- The metal complexes showed higher activity against bacteria and fungi strains than their parent ligands or $CoCl_2 \cdot 6H_2O$ and $NiCl_2 \cdot 6H_2O$, attributed to formation of the Schiff-base structure which increases the antimicrobial activity [33].
- Metal complexes of HL^1 have a higher degree of activity than the other complexes against all types of bacteria and fungi.
- Cobalt and nickel complexes of HL^1 and the cobalt complex of L^4 have an effect comparable with the standards *Chloramphenicol* and *Terbinafin* towards the tested organisms.

Table 5. Antimicrobial screening results of Schiff-base ligands and their metal complexes.

	Gram-positive bacteria		Gram-negative bacteria		Fungi	
Compound No.	*Staphylococcus aureus*	*Bacillus anthracis*	*Escherichia coli*	*Pseudomonas aeruginosa*	*Candida albicans*	*Penicillium italicum*
HL^1	20(51)	19(58)	16(53)	20(51)	15(42)	18(46)
$[CoL^1Cl(H_2O)_2] \cdot \frac{1}{2}H_2O$	27(69)	28(85)	29(97)	27(69)	27(75)	27(69)
$[NiL^1Cl(H_2O)_2] \cdot \frac{1}{2}H_2O$	38(97)	33(100)	27(90)	38(97)	28(78)	35(90)
L^2	13(33)	13(39)	12(40)	11(28)	10(28)	11(28)
$[CoL^2Cl(H_2O)]Cl \cdot H_2O$	25(64)	26(79)	21(70)	21(54)	22(61)	24(62)
$[NiL^2(Cl)_2(H_2O)_2] \cdot 1\frac{1}{4}H_2O$	22(56)	18(55)	20(67)	20(51)	20(56)	20(51)
HL^3	11(28)	12(36)	10(33)	10(26)	9(25)	9(23)
$[Co(HL^3)Cl(H_2O)]Cl \cdot \frac{1}{2}H_2O$	25(64)	26(79)	21(70)	19(49)	15(42)	19(49)
$[Ni(HL^3)(Cl)_2(H_2O)_2] \cdot \frac{1}{2}H_2O$	20(51)	20(61)	20(67)	19(49)	11(31)	18((46)
L^4	12(31)	13(39)	13(43)	11(28)	10(28)	10(26)
$[CoL^4(Cl)_2(H_2O)_2] \cdot 2\frac{1}{4}H_2O$	18((46)	21(64)	26(87)	26(67)	19(53)	19(49)
$[NiL^4(Cl)_2] \cdot \frac{1}{2}H_2O$	26(67)	22(67)	20(67)	25(64)	20(56)	18(46)
$CoCl_2 \cdot 6H_2O$	19(49)	17(52)	19(63)	18(46)	22(61)	13(33)
$NiCl_2 \cdot 6H_2O$	14(36)	20(61)	13(43)	15(38)	11(31)	17(44)
R.S.	39(100)	33(100)	30(100)	39(100)	36(100)	39(100)

Test done using the diffusion method.% activity index are in parentheses. R.S. – Reference standard: Chloramphenicol was used as a standard antibacterial agent; Terbinafin was used as a standard antifungal agent. Inhibition values: 6–13 low activity; 14–24 intermediate activity; 25–32 high activity; >32 very high activity.

- The electrolytic nature of the complexes sometimes enhance their activity as clear from comparison of the metal complexes of L^2 and HL^3 where inhibition zones of electrolytic cobalt complexes are greater than the non-electrolytic nickel complexes.

4. Conclusion

In this work, the choice of 4-amino-1,3 dimethyl-2,6 pyrimidine-dione to prepare our ligands is due to the fact that compounds containing pyrimidine have a broad spectrum of pharmacological activities. The structure of Schiff-base ligands and their cobalt(II) and nickel(II) complexes was confirmed by combination of elemental analysis, molar conductance, magnetic moment, thermal analysis and spectral data (IR, mass and solid reflectance). As a general conclusion, HL^1 is a monobasic tridentate ligand, while the other ligands (L^2, HL^3 and L^4) are neutral bidentate ligands. The chelation with the metal ions is brought about by the azomethine (N), carbonyl (O) and deprotonated phenolic (O). The geometry and mode of bonding in these complexes are reached based on infrared, electronic spectra and the magnetic susceptibility measurements to be octahedral, tetrahedral and square planar (figures 5–8, supplementary data available online). Additionally, the antimicrobial activity of the ligands and their complexes against different strains of bacteria and fungi show that the metal complexes possess remarkable biological activity and may serve as efficient therapeutic medicines.

References

[1] R. Hilal, Z.M. Zaky, S.A.K. Elroby. *Spectrochim. Acta A*, **63**, 740 (2006).
[2] Z.M. Zaki. *Spectrochim. Acta A*, **56**, 1917 (2000).
[3] S.I. Mostafa, M.A. Kabil, E.M. Saad, A.A. El-Asmy. *J. Coord. Chem.*, **59**, 279 (2006).
[4] H. Olmez, O.Z. Yesilel, H. Içbudak. *J. Therm. Anal. Calor.*, **63**, 105 (2001).
[5] H. Kiliç, M.L. Berkem. *J. Serb. Chem. Soc.*, **69**, 689 (2004).
[6] Z.H. Abd El-Wahab, M.M. Mashaly, A.A. Salman, B.A. El-Shetary, A.A. Faheim. *Spectrochim. Acta A*, **60**, 2861 (2004).
[7] M.M. Mashaly, Z.H. Abd El-Wahab, A.A. Faheim. *J. Chin. Chem. Soc.*, **51**, 901 (2004).
[8] M.M. Mashaly, Z.H. Abd El-Wahab, A.A. Faheim. *Synth. React. Inorg. Met.-Org. Chem.*, **34**, 229 (2004).
[9] Z.H. Abd El-Wahab, M.R. El-Sarrag. *Spectrochim. Acta A*, **60**, 271 (2004).
[10] G.G. Mohamed, Z.H. Abd El-Wahab. *Spectrochim. Acta A*, **61**, 1059 (2005).
[11] Z.H. Abd El-Wahab, M.M. Mashaly, A.A. Faheim. *Chem. Pap.*, **59**, 25 (2005).
[12] J. Bassett, R.C. Denney, G.H. Jeffery, J. Mendham. *Vogel's Textbook of Quantitative Inorganic Analysis*, 4th edn, Longmans, London (1978).
[13] M. Sönmez, A. Levent, M. Sekerci. *Russ. J. Coord. Chem.*, **30**, 655 (2004).
[14] M. Sönmez, A. Levent, M. Sekerci. *Synth. React. Inorg. Met.-Org. Chem.*, **33**, 1747 (2003).
[15] F.H. Urena, N.A.I. Cabeza, M.N.M. Carretero, A.L.P. Chamorro. *Transition Met. Chem.*, **26**, 160 (2001).
[16] K.K. Narang, V.P. Singh, D. Bhattacharya. *Transition Met. Chem.*, **22**, 333 (1997).
[17] M.S. Masoud, E.A. Khalil, A.M. Hindawy, A.M. Ramadan. *Can. J. Anal. Sci. Spectrosc.*, **50**, 207 (2005).
[18] M. Sönmez. *Polish J. Chem.*, **77**, 397 (2003).
[19] M. Sönmez, M. Sekerci. *Polish J. Chem.*, **76**, 907 (2002).
[20] G.G. Mohamed, Z.H. Abd El-Wahab. *Therm. Anal. Calor.*, **73**, 347 (2003).
[21] O.Z. Yesilel, H. Olmez. *Transition Met. Chem.*, **30**, 992 (2005).
[22] M.S. Masoud, E.A. Khalil, A.M. Hindawy, A.E. Ali, E.F. Mohamed. *Spectrochim. Acta A*, **60**, 2807 (2004).
[23] Z. Guoliang, F. Yunlong, W. Yihang. *J. Rare Earths*, **24**, 268 (2006).

[24] B.S. Garg, R.K. Sharma, E. Kundra. *Transition Met. Chem.*, **30**, 552 (2005).
[25] S. Chandra, L.K. Gupta. *Spectrochim. Acta A*, **61**, 1181 (2005).
[26] B.N. Figgis. *Introduction to Ligand Fields*, John Wiley and Sons, New York, London (1966).
[27] B.N. Figgis, R.S. Nyholm. *J. Chem. Soc.*, 12 (1954).
[28] P. Kamalakannan, D. Venkappayya. *J. Inorg. Biochem.*, **90**, 22 (2002).
[29] L.K. Gupta, S. Chandra. *Transition Met. Chem.*, **31**, 368 (2006).
[30] A.Z. El-Sonbati, A.A.M. Belal, S.I. El-Wakeel, M.A. Hussien. *Spectrochim. Acta A*, **60**, 965 (2004).
[31] V.P. Singh, P. Gupta. *J. Coord. Chem.*, **59**, 1483 (2006).
[32] U. El-Ayaan, A.A.M. Abdel-Aziz. *Eur. J. Med. Chem.*, **40**, 1214 (2005).
[33] T.T. Xu, X.Y. Xu, J. Gao, M.Y. Wang, L.D. Lu, J. Ni, G.X. Xu. *Synth. React. Inorg. Met.-Org. Nano-Met. Chem.*, **36**, 667 (2006).